South Eastern Australian
Climate initiative

Final report for **Project 1.5.1**

Application of the Bureau of Meteorology downscaling technique to coupled climate model simulation of the 20th century and implications for the attribution of observed climate change

Principal Investigator:
Dr. Bertrand Timbal, Centre for Australian Weather and Climate Research (CAWCR)
B.Timbal@bom.gov.au

Co-Authors:
Elodie Fernandez, (CAWCR) and Julie Arblaster, the National Center for Atmospheric Research, U.S.A. and CAWCR

CSIRO Land and Water
Ph: 02 6246 5617
seaci@csiro.au
http://www.seaci.org

Australian Government
Department of Climate Change
Bureau of Meteorology

MURRAY–DARLING BASIN AUTHORITY

State Government Victoria
Department of Sustainability and Environment

National Research FLAGSHIPS
Water for a Healthy Country
CSIRO

Initial Project objectives:

- Apply the statistical downscaling technique developed in project 1.3.1 to coupled climate model simulations of the 20th Century forced with several external forcings to evaluate the ability of climate models to capture large-scale changes which drive the observed regional changes.

- Draw conclusions about the extent to which the observed climate change is formally attributable to particular external forcings, either natural or anthropogenic.

Proposed methodology:

- The statistical technique will be applied to ensembles of simulations using different external forcings: natural only, anthropogenic only and natural and anthropogenic combined. Each ensemble is likely to have four or five members.

- The climate models used will be either the Parallel Climate Model (PCM) or the newer Community Climate System Model version 3 (CCSM3), both developed by NCAR in the U.S.A.

- The ability of the climate models to reproduce the large-scale changes will be assessed as well as the dependence of the model responses to the external forcing.

- The possibility of attributing observed changes to external forcing would follow suit.

Summary of the findings:

The analysis of the direct model outputs (DMOs) from the CCSM3 series of ensembles shows that:

- The model forced with natural external forcings has 1) no build up of surface pressure in autumn-winter-spring as observed, 2) small rainfall increases in these seasons and 3) no surface warming for either T_{min} or T_{max} all year around;

- The model forced with anthropogenic external forcing shows: 1) a build up of surface pressure which resembles the observed strengthening of the STR, 2) a significant surface warming for both T_{min} and T_{max} but 3) only a weak rainfall decline and mostly in winter rather than in autumn.

The downscaling of the CCSM3 ensembles has provided valuable, additional conclusions:

- The observed rainfall decline in autumn is outside the range of uncertainties (at least in parts of the SEACI domain) provided by the naturally forced ensemble;

- The mean response from the naturally forced ensemble pointed toward significant rainfall increases in autumn, winter and spring across south-eastern Australia (SEA) and therefore does not match the observations;

- In contrast, the two ensembles forced with anthropogenic forcings alone, and combined with natural forcing, point toward rainfall declines in the last 20 years: large in autumn, small in spring and very small in winter;

- The largest rainfall decline is most often obtained from the ensemble combing both natural and anthropogenic external forcings (rather than anthropogenic alone) but remains smaller

than the largest observed declines (e.g. only about 50 per cent in autumn) but comparable to observed values in other seasons;

- The downscaling of CCSM3 provides a more definitive attribution of the on-going surface warming across SEA for both T_{max} and T_{min} as the most recent trends in temperature are outside the 90 per cent range of uncertainty obtained from the naturally forced ensemble. In contrast, the fully forced ensemble extended to 2008 using the A2 scenario matches the observed temperature trends very well.

Technical details

Update on methodology and preliminary comments

Following the completion of project 1.4.1, the National Climate Atmospheric Research (NCAR) laboratory was approached to obtain the most up to date set of data to use in project 1.5.1. In the past, a series of ensembles from the Parallel Climate Model (PCM) were used to perform a similar attribution of the rainfall decline in the south-west of Western Australia (Timbal et al., 2006; Timbal and Arblaster, 2007). One of the issues faced during that work was that not all the predictors needed were available from the NCAR archived results. Recently, similar externally forced ensembles of simulation were performed with a newer climate model: the Community Climate System Model version 3 (CCSM3, Collins et al., 2006). While the limitations regarding the list of predictors we wanted to use remain, it was thought preferable to source this new set of data from the model currently being developed by NCAR. Overall, the framework used by NCAR to perform these simulations is very well suited to this formal attribution study. The model is run with well defined external forcings separated in two groups:

1. anthropogenic - which includes greenhouse gases, aerosols and stratospheric ozone;

2. natural – which includes variations of the solar constant and volcanic eruptions; and

3. both natural and anthropogenic forcings combined (Meehl et al., 2006).

Each ensemble consists of five simulations with slightly different initial conditions (starting around 1850) enabling an estimation of the uncertainty of the climate signals. All 20th Century simulations were run until the end of 1999.

In this report, the ability of each ensemble to reproduce observed climatic trends both for temperature and rainfall in the SEA is evaluated. Direct Model Outputs (DMOs) are used as well as results from the statistical downscaling of the three ensembles using the Bureau of Meteorology (BoM) Statistical Downscaling Model (SDM) adapted to the surface climate data selected for the SEACI program during project 1.1.1 (Timbal and Murphy, 2007), and during project 1.3.1 (Timbal et al., 2008). The ability of the SDM to reproduce on-going climatic trends was assessed in project 1.4.1 and found suitable (Timbal and Fernandez, 2009). Results are shown for two climate entities: the South-West of Eastern Australia (SWEA) and the Southern Murray-Darling Basin (SMD).

The optimal combination of predictors for each SDM had to be modified to match the existing dataset available in the CCSM3 archive stored at the NCAR, USA (Table 1). In particular Q_{850} was not available and was, in general, replaced by the model precipitation. In addition T_{max} and T_{min} were not archived for the all forcing simulations and hence could not be used for all cases. To prevent mismatches in the application of the SDM to CCSM3 simulations both T_{max} and T_{min} were replaced by T_{850} whenever needed. In the case of rainfall, the only modification required affects

the downscaling for SWEA in autumn, where Q_{850} is replaced by PRCP which, as a single predictor, was producing a smaller rainfall trend (Fig. 2 in Timbal and Fernandez, 2009) and T_{max} was replaced by T_{850} which was producing similar trends. Overall the modified SDM is expected to reproduce only slightly less of the rainfall trends as the single most important predictor is Mean Sea Level Pressure (MSLP) (see Fig. 2 in Timbal and Fernandez, 2009). In the case of the downscaling for T_{max}, in the few instances where T_{max} had to be replaced by T_{850}, it is not expected to downgrade the results as in most instances T_{850} as a single predictor was producing a larger temperature trend which was more similar to the observations. Similarly for T_{min}, the changes are not anticipated to significantly impact on the SDM's ability to reproduce observed changes.

Analysis of large-scale predictor changes in the 20th century simulations

The large-scale changes simulated by CCSM3 during the 20th century were investigated by looking at 30-year and 50-year linear trends as well as differences between the last 30 years (1970 to 1999) and the earlier part of the 20th Century (1900 to 1969). While the linear trends are fairly robust (the 30-year and 50-year trends were often similar (not shown), they are often noisier and harder to interpret. Therefore, in this report, only maps of differences between the two periods are shown.

Earlier research during SEACI demonstrates that the rainfall decline in SEA is linked to the build up of mean sea level pressure (MSLP) above southern Australia (Timbal et al., 2008). The rise in MSLP above southern Australia is well documented (Timbal and Hope, 2008) and, since it is one of the most important large-scale predictors used in the statistical downscaling of rainfall, T_{max} and T_{min} across SEA, it is appropriate to analyse how the CCSM3 modelled MSLP response to external forcings (Fig. 1 to 4). The natural ensemble displays anomalies in the latter period of the 20th century which are of small magnitude (mostly below 0.2 hPa) and which, if anything, are rather negative (in summer and winter) above SEA. In autumn and spring, anomalies are slightly positive (about 0.1 hPa) above SEA. Overall there is no large-scale build-up of MSLP around Australia in the CCSM3 mean ensemble forced with natural external forcings. In contrast, the ensemble mean in the case of anthropogenic forcings exhibits a clear and consistent (across all four seasons) build up of MSLP above southern Australia. This feature resembles future projections of MSLP due to increases in greenhouse gases (Fig. 10.9 p 767, in the IPCC 4th assessment, Solomon et al., 2007). The structure of the MSLP increase is mostly zonal with largest values south of the continent (up to 1 hPa at 45° to 50°S). Above SEA, the largest signal is in winter (+0.4 to 0.6 hPa) and spring (0.2 to 0.5 hPa) and is weaker in summer and autumn (0 to 0.2 hPa). Finally, the last ensemble mean, where the CCSM3 model was forced by natural and anthropogenic forcings combined, displays very similar patterns to the anthropogenic ensemble. This indicates that the anthropogenic forcings are therefore the most important source of the simulated differences during the late 20th century. Above SEA, the signal is larger for the combined forcings than for anthropogenic forcings alone in winter (up to 0.8 hPa) and autumn, unchanged in summer and weaker in spring. Those small differences (i.e. larger signal in autumn, smaller signal in spring) make it the ensemble mean which most closely match the observed MSLP trends, based on HadSLP2 data (Allan and Anselm, 2006).

In addition to the MSLP response to external forcings, the direct model output (DMO) for rainfall was also evaluated. This is important for two reasons:

1. to evaluate the possibility of attributing the observed rainfall decline directly without using the BoM SDM; and

2. to understand the downscaled rainfall response in the modified version of the BoM SDM, given that the DMO rainfall is the second most important predictor in the SDM (after MSLP).

Overall, the rainfall difference maps (Fig. 5) are noisier, with more complex structures and harder to interpret, than the MSLP difference maps. The mean of the natural ensemble suggests a decline of summer rainfall across the Australian continent, strongest in the north but also across SEA, while in autumn and winter, the model suggests a small increase. The response of the anthropogenic ensemble is rather different: an increase of summer rainfall, a decrease in autumn above large part of eastern Australia, including SEA, and a decrease confined to southern Australia (south-west of Western Australia (SWWA) and south-west of eastern Australia (SWEA), two regions which have been identified as having linked rainfall variability (Hope et al., 2009). Finally, as per MSLP, the full forcing ensemble is more closely aligned with the anthropogenic ensemble than the natural one. For the full forcing ensemble, the autumn rainfall decline is now shifted more across central Australia (and hence is less realistic for SEA), while the winter rainfall decline is more widespread (and hence more realistic).

The other two surface variables worth investigating are T_{max} (Fig. 6) and T_{min} (Fig. 7). As per rainfall, they are both an interesting DMO and temperature is an important predictors for the statistical downscaling of the CCSM3 ensembles. As noted earlier, T_{max} and T_{min} are not available for the all forcings ensemble, but since a clear contrast is visible between the natural ensemble and the anthropogenic ensemble, and following the case of MSLP and rainfall, it is reasonable to expect that the response in the all forcing simulations is close to the anthropogenic ones. Overall, with natural forcings, there is hardly any warming across the Australian continent for both T_{max} and T_{min}. The only case with a warming above 0.2 °C is T_{max} in summer; in all other cases there is either no signal or a small cooling. In contrast, the mean of the ensemble forced with anthropogenic forcings displays a consistent (across all cases) warming; the structure and amplitude of which varies from season to season. Across SEA, it ranges from 0.2 to 0.4 °C and is strongest in autumn and spring for both T_{max} and T_{min}. In general the model produces a stronger warming for T_{min} than T_{max}.

In addition to the mean ensemble signal, it is necessary to evaluate the consistency of the climate signal within each ensemble by looking at individual simulations (five were available for all three ensembles). This is illustrated for MSLP changes in autumn by showing, for each ensemble, two simulations with the most contrasted signals: the lowest MSLP increase (left column in Fig. 8) and the strongest surface build up (right column). In all three ensembles, the spread is quite large. For the natural ensemble, MSLP is either declining by up to 0.2 hPa across SEA or increasing by the same amount. For the two other ensembles (anthropogenic and full forcings), all simulations exhibit a MSLP increase which is mostly zonal, with the largest values further south. However, the magnitude of the increase is quite different and leads to very different MSLP anomalies above SEA ranging from slightly negative (-0.1 to -0.2 hPa) to strongly positive (ranging from 0.3 to 0.7 hPa across SEA) in the case of the anthropogenic forcing. In the simulations for anthropogenic and natural forcings combined, the uncertainties of the response resemble those of the anthropogenic ensemble but with smaller scatter. A similar analysis was conducted for the surface variables (rainfall, temperature). As expected, due to the noisy nature of rainfall, the uncertainties in all three ensembles are very large and there is overlap between the ensembles (not shown). In contrast, for both T_{max} and T_{min}, individual simulations from the two ensembles show a more consistent signal, suggesting a significant difference between the two ensembles.

In order to better assess the significance of the simulated changes by each ensemble and to compare them with observed changes across the SEACI area, results were averaged across SEA and are shown over the century long simulations. Fig. 9 shows how well the model has captured the observed variability of MSLP over a large domain around SEA (between 120° and 160°E and 20 and 50 °S, this is a larger domain than for SEA rainfall as MSLP has more spatial coherence) during the 20th Century. The black solid line depicts the observational estimate based on HadSLP2 dataset (Allan and Anselm, 2006). It is a 20-year running average from 1900 to 2008 with the

century mean removed. The blue lines represent the 75 per cent confidence interval for the same value from the natural ensemble. The confidence interval was estimated using:

$$\mu \pm 1.96 \times [1 + (1/\sqrt{N})] * \sigma \quad \text{Where}$$

μ is the ensemble mean of the 20-year running average of the natural ensemble, and
σ is estimated using seasonal means from the 5 simulations over the same 20 years.

The same confidence interval is shown for the anthropogenic (red lines) and full forcing ensembles (green lines), one panel per calendar season. All 20th Century simulations were run until 1999 and, hence, the 20-year running mean stops in 1990. Because, the fully forced simulations were used by NCAR as the starting point for the 21st Century future projections using IPCC emission scenarios, we used the first 10 years of the simulations forced with the A2 scenario, which is very close to the observed emissions from 2000 to 2008, to extend the full forcings ensemble to 2008.

Similar results are depicted for rainfall (Fig. 10), where rainfall is averaged over continental points of Australian mainland south of 33.5 °S and East of 135 °E (our definition of SEA) and compared with the Bureau of Meteorology National Climate Centre (NCC) 0.25° gridded rainfall from the same region. Fig. 11 and Fig. 12 show the same results for T_{max} and T_{min}, for which seasonal means of the observations over SEA are only available from 1950.

Starting with MSLP, it is difficult to rule out any observed values as being outside the range of uncertainties of any particular ensemble. Even the most dramatic observed feature, the rise of MSLP in autumn from the 1960s to now is mostly within the uncertainty range of all three ensembles. The lowest value in the 1960s was slightly outside the range of all three ensembles and the most recent highest value on record appeared to be outside the range of the natural ensemble, just within the 75 per cent limit of the anthropogenic forcings and within the range of the full forcings ensemble. This confirms the indication given by the mean of the ensemble results that the MSLP increase in autumn is best captured by the full forcings ensemble, but even the natural forcings ensemble cannot be totally ruled out as it is expected that observations from time to time (25 per cent over a century) would fall outside a 75 per cent confidence interval. The MSLP increase in summer is also more consistent with the full forcings ensemble; the anthropogenic forcings gives a stronger rise in the last 20 years than the observations and the natural forcings ensemble suggests declining values of MSLP. In winter and spring, the observed MSLP variability above SEA is consistent with any of the three ensembles.

Not surprisingly for rainfall, a very noisy variable, the observed curve is often reaching the 75 per cent limit of all the ensembles. In particular the very high rainfall of the 1960s to 1980s appears to be just at the limit of all three ensembles (most noticeably in spring). The recent low values in autumn as well as the low values in the 1930s and 1904s in winter and spring are beyond the 75 per cent uncertainty level of all three ensembles. During the middle of the century, no particular ensemble appears to be lower than the other one. On the contrary, for the recent decline in autumn, the anthropogenic forcings and, more importantly, the full forcings ensemble extended into the beginning of the 21st Century using scenario A2 does suggest a significant rainfall decline, albeit not as large as observed.

For surface temperature, no attempt was made to extend results beyond the end of the 20th Century as only natural and anthropogenic ensembles were available. In almost all cases, by the end of the century, the overlap between the two ensembles is being reduced as the anthropogenic ensemble starts to track significantly higher. However, by the end of the 20th Century, none of the observed temperature anomalies across SEA are outside the 75 per cent range of any ensemble. All black curves are getting close to the upper limit of the natural ensemble (most notably for T_{min}) and it is likely that the recent rapid rise at the beginning of the 21st century for T_{max} would

push the limit of the natural ensemble if the simulation was continued during the last decade. But in the absence of the values for the early part of the 21st Century, it is not possible to definitely attribute the observed trends of the late 20th Century to external forcings.

Following on the analysis of the CCSM3 DMOs, we will now look at the results of the statistical downscaling of the same three ensembles of simulations.

Reproduction of the drying trends across SEA using statistical downscaling

The BoM SDM was applied to daily outputs from the five simulations of the three ensembles with the CCSM3 model using the modified version of the optimised SDM to deal with the data limitation discussed earlier (Table 1). In order to assess the ability of the downscaled model simulations to reproduce the observed rainfall trends, linear trends were calculated on a shorter (1980-1999) and a longer (1960-1999) period and averaged across the 324 rainfall stations used in the two climate entities: SWEA (Table 2) and SMD (Table 3) and for all four calendar seasons. For each ensemble, and using the two periods, the ranges of the linear trends are provided as well as the ensemble mean. In addition, histograms of the linear trends are presented (Fig. 13). The histograms are made of 30 cases for each ensemble: five simulations time six different SDMs. The histograms show the linear trends for the shorter periods, because, despite the higher uncertainties, they better capture the magnitude of the recent rainfall decline across SEA which is obvious in most seasons and regions in the trends calculated since 1980. It is worth noting that although, the rainfall decline across SEA is generally measured since 1996 (Timbal and Murphy, 2007) (at which time there was an apparent step change in the annual rainfall series), it is clear from the observed seasonal rainfall series shown earlier (Fig. 10) that in autumn, winter and spring, rainfall across SEA has been declining since the early 1980s. Starting from a higher than normal base at the end of the very wet 1960s and 1970s, the average rainfall has only fallen below the long-term average since the mid 1990s. In terms of linear trends, negative linear trends are consistently obtained for any period since 1980.

The most significant feature is the autumn rainfall decline (larger in SWEA than in SMD). A key finding is that the observed autumn rainfall decline is outside the range of linear trends from the statistical downscaling of the natural ensemble, while it is not outside the range from the other two ensembles, although the negative mean trends in both ensembles are lower than the observed value. The histogram shows the large uncertainties for all three ensembles and the tail of the distribution encompasses the observed value for the anthropogenic and full forcing ensembles. Contrary to the SWEA, in SMD where the observed trend is slightly less, and the spread amongst ensembles even larger, the observed value is not outside the range obtained from the downscaling of the natural ensemble. But, as is the case for SWEA, only the anthropogenic and full forcings ensembles have mean negative trends, and the full forcing ensemble is the closest to the observed trend.

In winter, in both SWEA and SMD, results are very similar to autumn, with the natural ensemble suggesting a rainfall increase while the full forcings ensemble is the most realistic of the three, but the observed trends cannot be ruled out from any ensemble. In spring, all three ensembles are very consistent with the winter signal: a rainfall increase with the natural ensemble, a small decrease with the anthropogenic forcing and a bigger decrease with the full forcing. However, no rainfall decrease has been observed in spring during the 1980–1999 periods. It is only in the latest decades that spring rainfall in SEA has started to decline: in SWEA the linear trend for the observations from 1980-2008 is -0.19 mm.day^{-1} per century accelerating during 1990–2008 to -3.39 mm.day^{-1} per century. Finally, the observed rainfall increase in summer is better captured by the natural and the full forcings ensembles and less by the anthropogenic forcings ensemble (i.e. in SMD, the observed trend is outside the uncertainty range of the anthropogenic ensemble).

Reproduction of the warming trends across SEA using statistical downscaling:

The BoM SDM was also applied to generate daily local temperatures at 41 locations across SEA. The optimised SDM was adapted to deal with data availability from the CCSM3 archive (Table 1). As per rainfall, linear trends were calculated on the reconstructed series for 1960-1999 and 1980-1999 and averaged for the two regions of interest: SWEA and SMD for T_{max} (Table 4 and 5) and T_{min} (Table 6 and 7). In contrast to rainfall, the on-going warming is seen in the observational record from earlier on. As a consequence, as the longer term trends are more stable, we will focus on the linear trends calculated from 1960 to 1999. Accordingly the histograms of the trends calculated from the 30 cases for each ensemble are shown for this 40 years period (Figure 12 and 13).

Downscaled results, here, are very consistent with the DMOs results discussed earlier. In general, the significance is increased as, in many instances, the observed trends are outside the range of uncertainties calculated from the natural ensemble. This is the case for T_{min} in summer in both regions, and in winter and spring in SWEA, for T_{max} in both regions in summer and winter, and in autumn and spring in SWEA. In contrast, the observed trends are almost always within the range of uncertainties obtained from the downscaling of the full forcings ensemble. In all cases, the best match is obtained from the full forcings ensemble: the mean of this ensemble is closer to the observed values than any other ensemble mean (in all cases for T_{max} and in most cases for T_{min} although there are a few instances where the mean from the anthropogenic ensemble is closer to the observed value). The observed value is nearly always within the range of uncertainties obtained form the downscaling of the full forcing ensemble (the sole exception is winter in SWEA). From that set of results, it is very clear that natural forcings alone are not sufficient to explain the observed warming across SEA. And while anthropogenic forcings alone provide good estimates, the full forcings provide the best match. This last result cannot be verified with DMOs as surface data (T_{max} and T_{min}) are not available for this ensemble.

Since all ensembles can be compared using the downscaling results, it was found interesting to redo the century long evolutions of the uncertainties of each ensemble (shown for DMOs in Fig. 10 to 12) using the downscaled stations results averaged across the entire SEA (Fig. 16 and 17). The overall picture for rainfall is not much different (not shown) apart from rainfall in autumn where the current decline is clearly within the uncertainty range of the full forcings ensemble while stretching the bound of uncertainties of the other two ensembles. For temperature, the new graphs show the improvement resulting from using statistical downscaling versus DMOs. The statistical downscaling of the CCSM3 ensemble provides a narrower band of uncertainties than DMOs, and for this reason, the uncertainties bands in Fig. 16 and 17 are now calculated using the 90 per cent confidence interval instead of 75 per cent. The fact that the observations in the most recent decade are often sitting at the edge of the natural ensemble uncertainty range (upper blue line) is therefore even more convincing evidence that the most recent warming observed across SEA is not consistent with natural forcings alone. In addition, we were able to obtain downscaled value for the full forcings ensemble and its continuation into the early 21st century using the A2 emissions scenario (green lines). Even during the first decade of the 21st century, the downscaling of the CCSM3 model forced with full forcings tracks the observations very well, including the recent acceleration of warming for T_{max} due to the on-going drought, as well as the T_{min} reduction in autumn due which is also contributed to by the rainfall anomaly in that season.

Conclusions

The application of the Bureau of Meteorology Statistical Downscaling Model to simulations of the 20th Century with the NCAR CCSM3 climate model externally forced with natural and anthropogenic external forcings has permitted a full attribution study of the observed surface climate changes (temperature and rainfall) across south-eastern Australia. Alongside the analysis

of the direct model outputs, the application of the SDM has provided additional information, and in some instances a clearer picture, which allows ruling out natural forcings as a possible explanation for some of the observed trends, namely:

1. most of the observed surface warming; and

2. the large autumn rainfall decline observed in the south-west of Eastern Australia.

Overall, the large-scale changes important to an understanding of the observed changes in SEA climate are better represented by the CCSM3 model when a full set of forcing (combining natural and anthropogenic forcings) is used. In many instances, most of the signal is already captured using anthropogenic forcings alone, but a more realistic behaviour is observed with both set of forcings.

Acknowledgement

This work was funded by the South Eastern Australia Climate Initiative. Thanks are due to the NCAR for making the CCSM3 outputs available and to Gary Strand for providing the data.

References

- Allan, R. and Ansell, T., 2006: A newly globally complete monthly historical gridded mean sea level pressure dataset (HadSLP2): 1850-2004, *J Climate*, **19**, 5816–5842.

- Solomon S., D. Qin, M. Manning, Z. Chen, M. Marquis, K. Averyt, M. Tignor, and H.M. Miller (eds.), 2007: "Climate Change 2007: The Physical Science Basis", contribution of Working Group I to the Fourth Assessment Report of the Intergovernmental Panel on Climate Change, Cambridge University Press, Cambridge, NY, USA, 996 pp.

- Hope, P., B. Timbal and R. Fawcett, 2009: "Associations between rainfall variability in the southwest and southeast of Australia and their evolution through time", Int. J. of Clim. (accepted).

- Collins, W. D., and Co-authors, 2006: The Community Climate System Model version 3 (CCSM3). J. Climate, **19,** 2122–2143.

- Meehl, G. A., W. M. Washington, B. D. Santer, W. D. Collins, J. M. Arblaster, A. Hu, D. Lawrence, H. Teng, L. E. Buja, and W. G. Strand (2006), Climate change projections for twenty-first century and climate change commitment in the CCSM3, J. Clim., **19**, 2597–2616.

- Timbal, B. and J. Arblaster, 2006: "Land covers change as an additional forcing to explain the rainfall decline in the South West of Australia". *Geo. Res. Let.*, 33, L07717, doi:10.1029/2005GL025361.

- Timbal, B., J. Arblaster and S. Power, 2006: "Attribution of the late 20th century rainfall decline in South-West Australia". *J. of Climate*, 19(10), 2046-2062.

- Timbal B. and B. Murphy, 2007: "Document changes in south-eastern Australian rainfall, temperature, surface humidity and pan evaporation". South-Eastern Australian Climate Initiative (SEACI), final report for project 1.1.1, 19 pp.

- Timbal, B., B. Murphy, K. Braganza, H. Hendon, M. Wheeler and C. Rakich, 2007: "Compare documented climate changes with those attributable to specific causes". South-Eastern Australian Climate Initiative (SEACI), final report for project 1.1.2, 19 pp.

- Timbal, B. and P. Hope, 2008: "Observed early winter Mean Seal Level Pressure changes above southern Australia: a comparison of existing datasets", *CAWCR res. Let.*, **1**, 1-7.

- Timbal, B., B. Murphy, E. Fernandez and Z. Li, 2008: "Development of the analogue downscaling technique for rainfall, temperature, surface humidity and pan evaporation". South-Eastern Australian Climate Initiative (SEACI), final report for project 1.3.1, 17 pp.

- Timbal, B. and E. Fernandez, 2009: "Application of the Bureau of Meteorology downscaling technique to reanalyses: implications for the attribution of observed climate change. South-Eastern Australian Climate Initiative (SEACI), final report for project 1.4.1, 21 pp

Appendix: figures and tables

Table 1: *Optimum and modified combinations of predictors, for 4 calendar seasons, the 3 predictands in 2 regions: SWEA and SMD. The predictors are: MSLP is the Mean Sea Level Pressure; T_{max} and T_{min} are the surface min and max temperature; PRCP is the total rainfall; Q is the specific humidity; R is the relative humidity; T is the temperature; U and V are the zonal and meridional wind components; and subscript numbers indicates the atmospheric level for the variable in hPa. Predictors which had to be modified are indicated with bold font.*

Season		SWEA		SMDB	
		Optimum	Modified	Optimum	Modified
$\mathbf{T_{max}}$	DJF	MSLP & T_{850}	MSLP & T_{850}	MSLP & $\mathbf{T_{max}}$	MSLP & $\mathbf{T_{850}}$
	MAM	MSLP & $\mathbf{T_{max}}$	MSLP & $\mathbf{T_{850}}$	MSLP & $\mathbf{T_{max}}$	MSLP & $\mathbf{T_{850}}$
	JJA	MSLP & T_{850} & $\mathbf{T_{max}}$ & U_{850}	MSLP & T_{850} & U_{850}	MSLP & T_{850} & $\mathbf{T_{max}}$ & U_{850}	MSLP & T_{850} & U_{850}
	SON	MSLP & T_{850}	MSLP & T_{850}	MSLP & T_{850} & U_{850}	MSLP & T_{850} & U_{850}
$\mathbf{T_{min}}$	DJF	MSLP & T_{850}	MSLP & T_{850}	T_{850} & $\mathbf{Q_{850}}$	T_{850} & **PRCP**
	MAM	MSLP & T_{850} & $\mathbf{Q_{850}}$	MSLP & T_{850} & **PRCP**	T_{850} & $\mathbf{Q_{850}}$	T_{850} & **PRCP**
	JJA	MSLP & T_{850} & $\mathbf{Q_{850}}$	MSLP & T_{850} & **PRCP**	MSLP & T_{850} & $\mathbf{Q_{850}}$	MSLP & T_{850} & **PRCP**
	SON	MSLP & T_{850} & $\mathbf{Q_{850}}$	MSLP & T_{850} & **PRCP**	MSLP & T_{850} & $\mathbf{Q_{850}}$	MSLP & T_{850} & **PRCP**
Prec	DJF	MSLP & PRCP & T_{850}	MSLP & PRCP & T_{850}	MSLP & PRCP & V_{850}	MSLP & PRCP & V_{850}
	MAM	MSLP & $\mathbf{T_{max}}$ & $\mathbf{Q_{850}}$ & U_{850}	MSLP & $\mathbf{T_{850}}$ & **PRCP** & U_{850}	MSLP & PRCP & V_{850}	MSLP & PRCP & V_{850}
	JJA	MSLP & PRCP & V_{850}	MSLP & PRCP & V_{850}	MSLP & PRCP & V_{850}	MSLP & PRCP & V_{850}
	SON	MSLP & PRCP	MSLP & PRCP	MSLP & PRCP & V_{850}	MSLP & PRCP & V_{850}

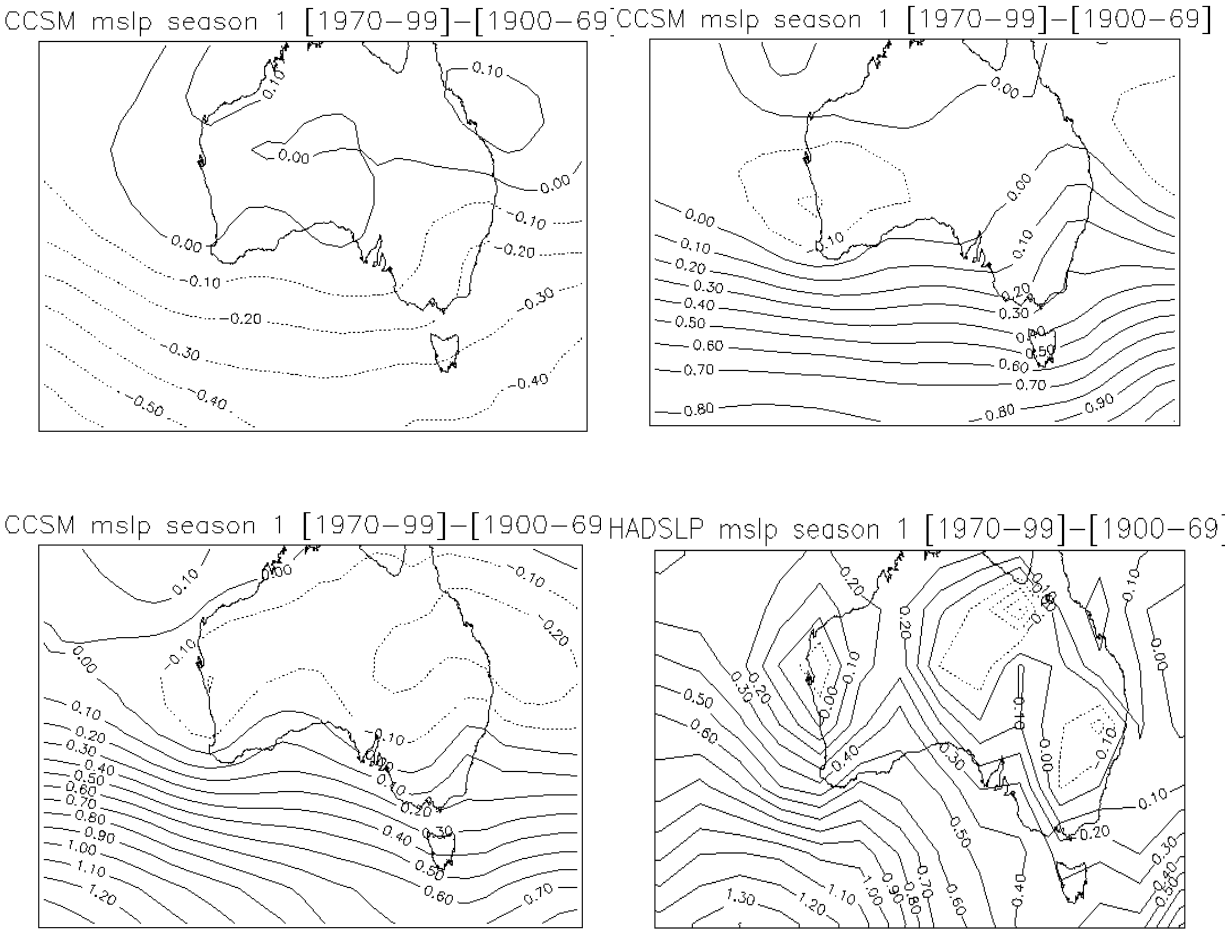

Fig 1: *Maps of differences of summer MSLP (in hPa) between 1970-1999 and 1900-1969, for the natural (top left), anthropogenic (top right), and all forcings (bottom left) ensemble means and for the HadSLP2 dataset (bottom right).*

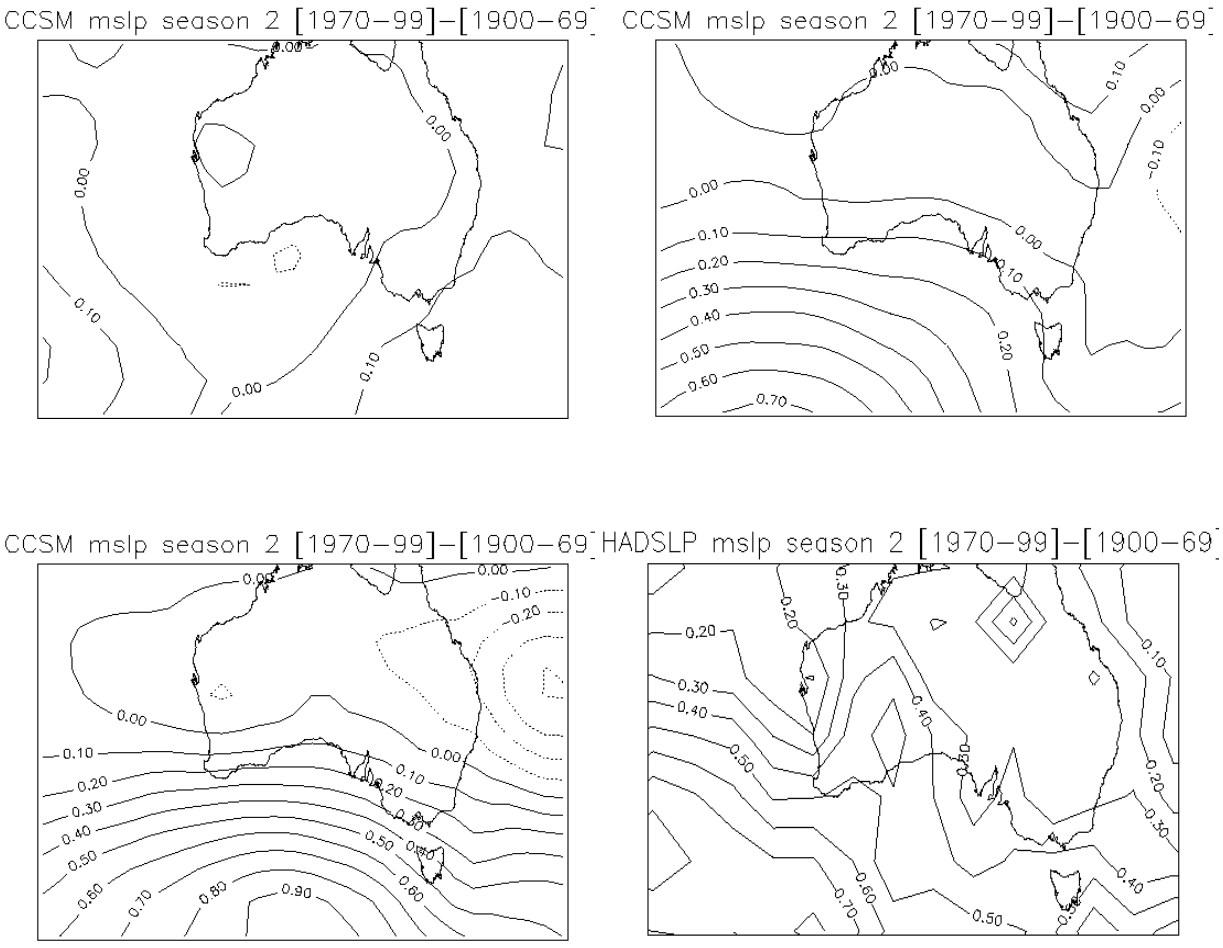

Fig 2: *As per Figure 1 but for autumn.*

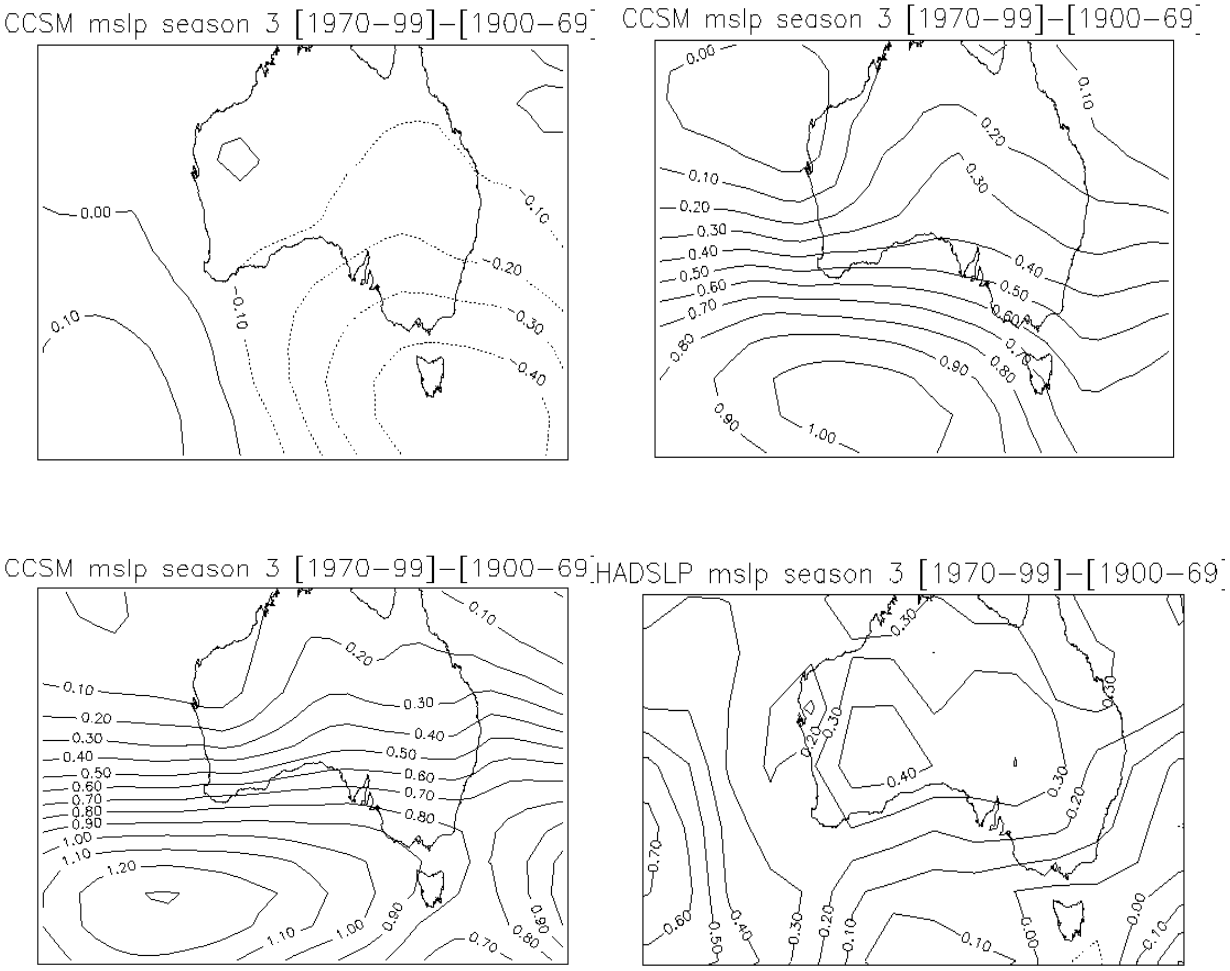

Fig 3: *As per Figure 1 but for winter.*

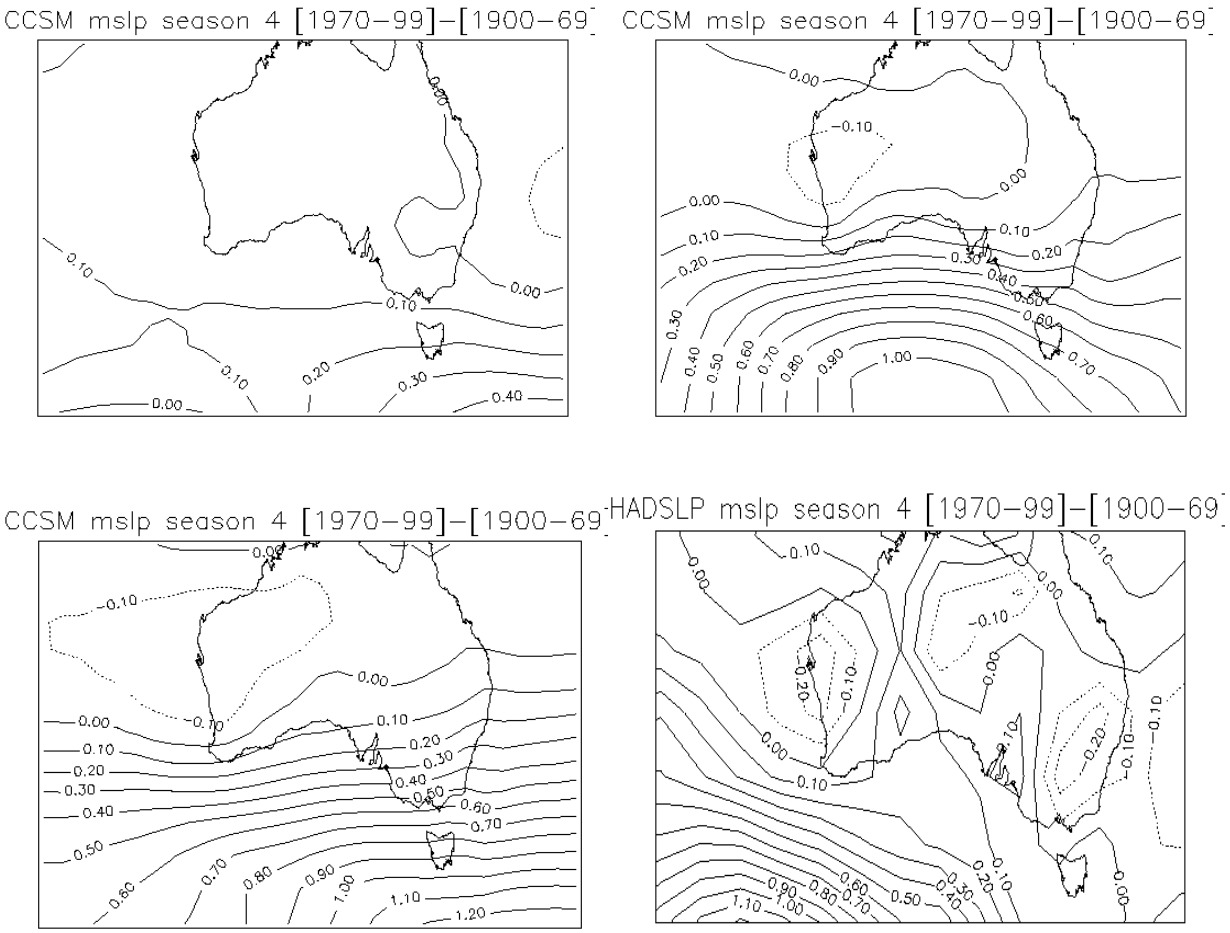

Fig 4: *As per Figure 1 but for spring.*

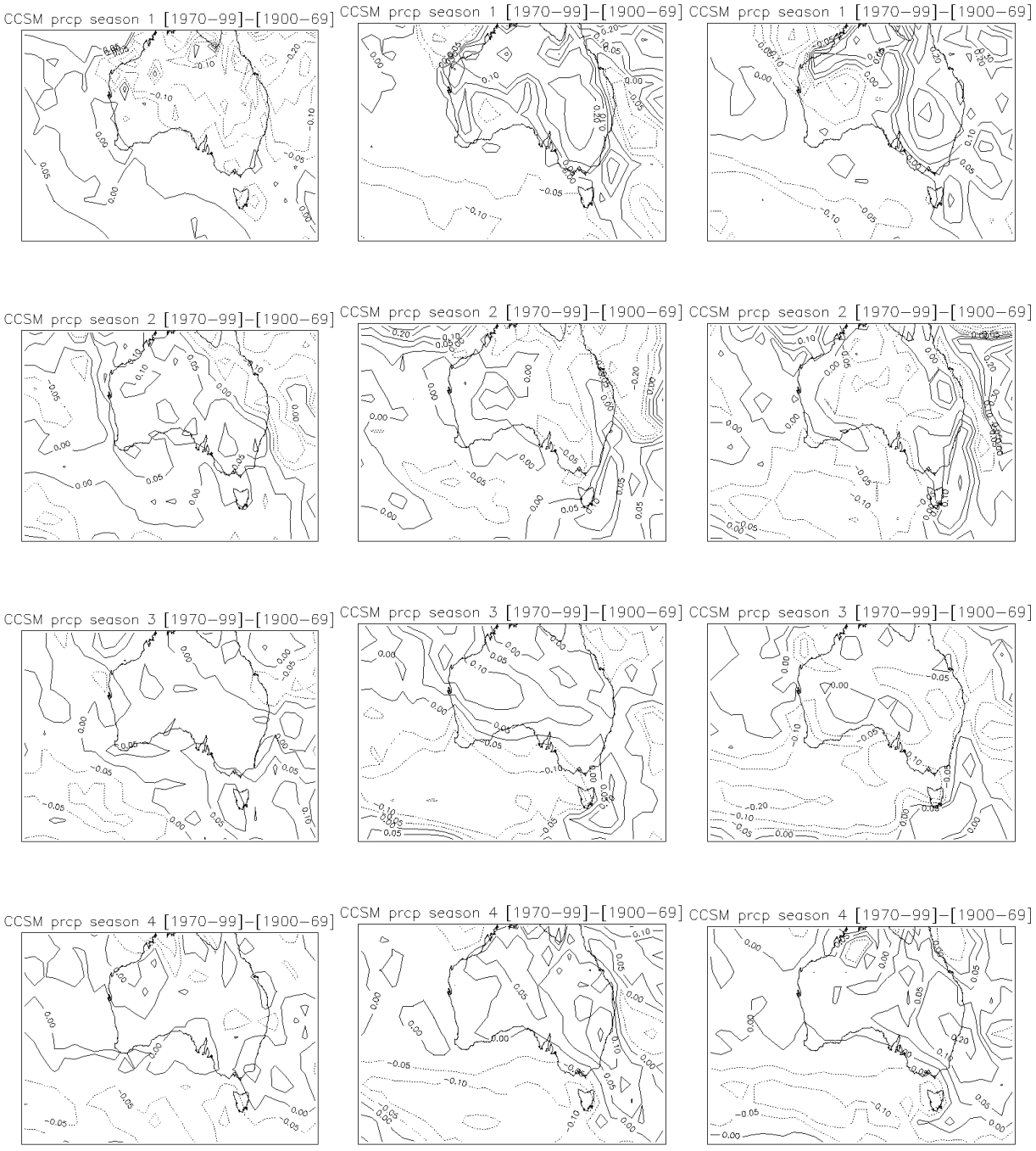

Fig 5: *Maps of differences in rainfall (mm.day^{-1}) between 1970-1999 and 1900-1969, for the natural (left), anthropogenic (middle), and all forcings (right column) ensemble means. Each row shows a season: summer, autumn, winter and spring from top to bottom.*

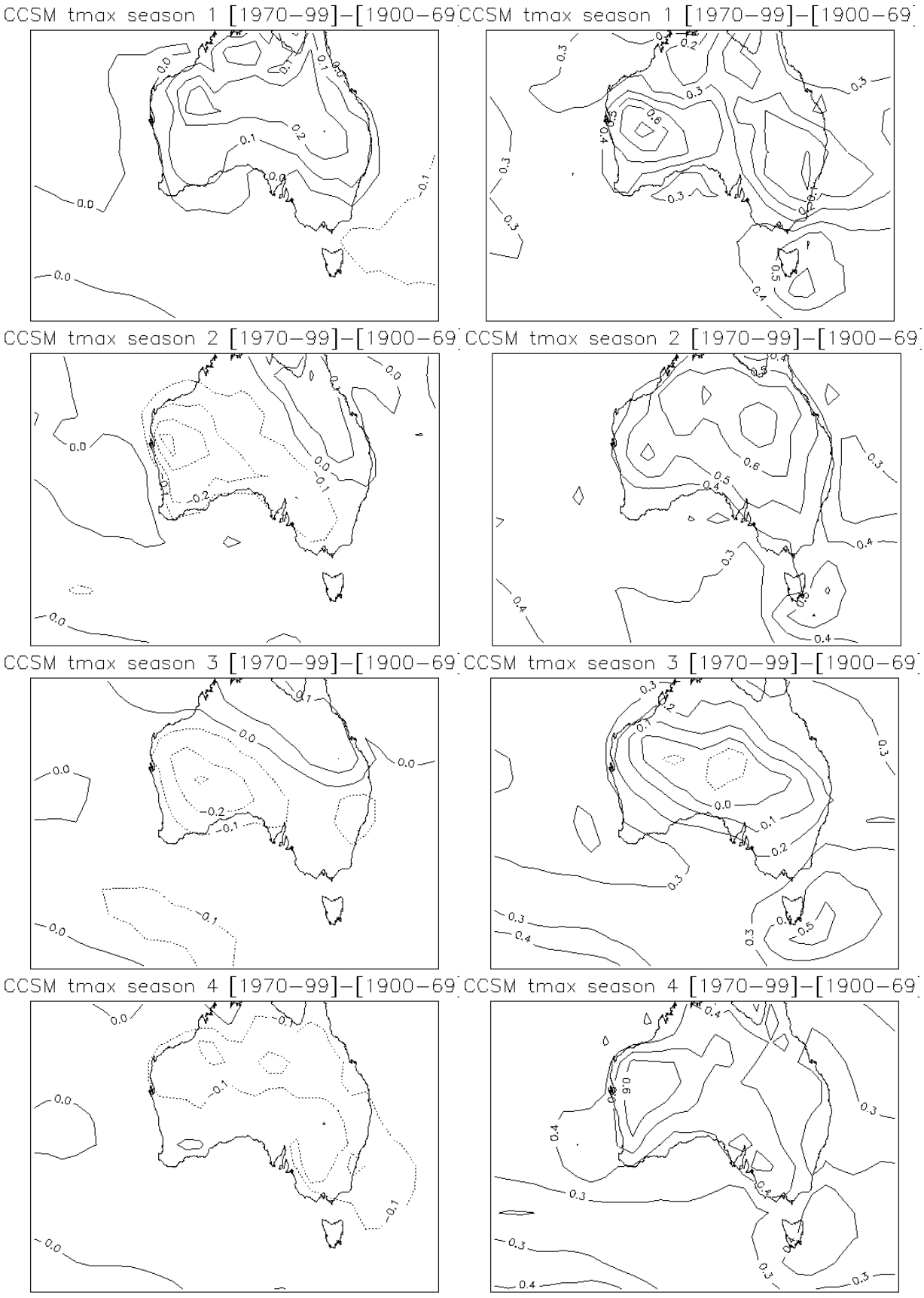

Fig 6: *As per Figure 5 but for maximum Temperature (T_{max}) in °C. The natural (left) and anthropogenic (right) ensembles are shown.*

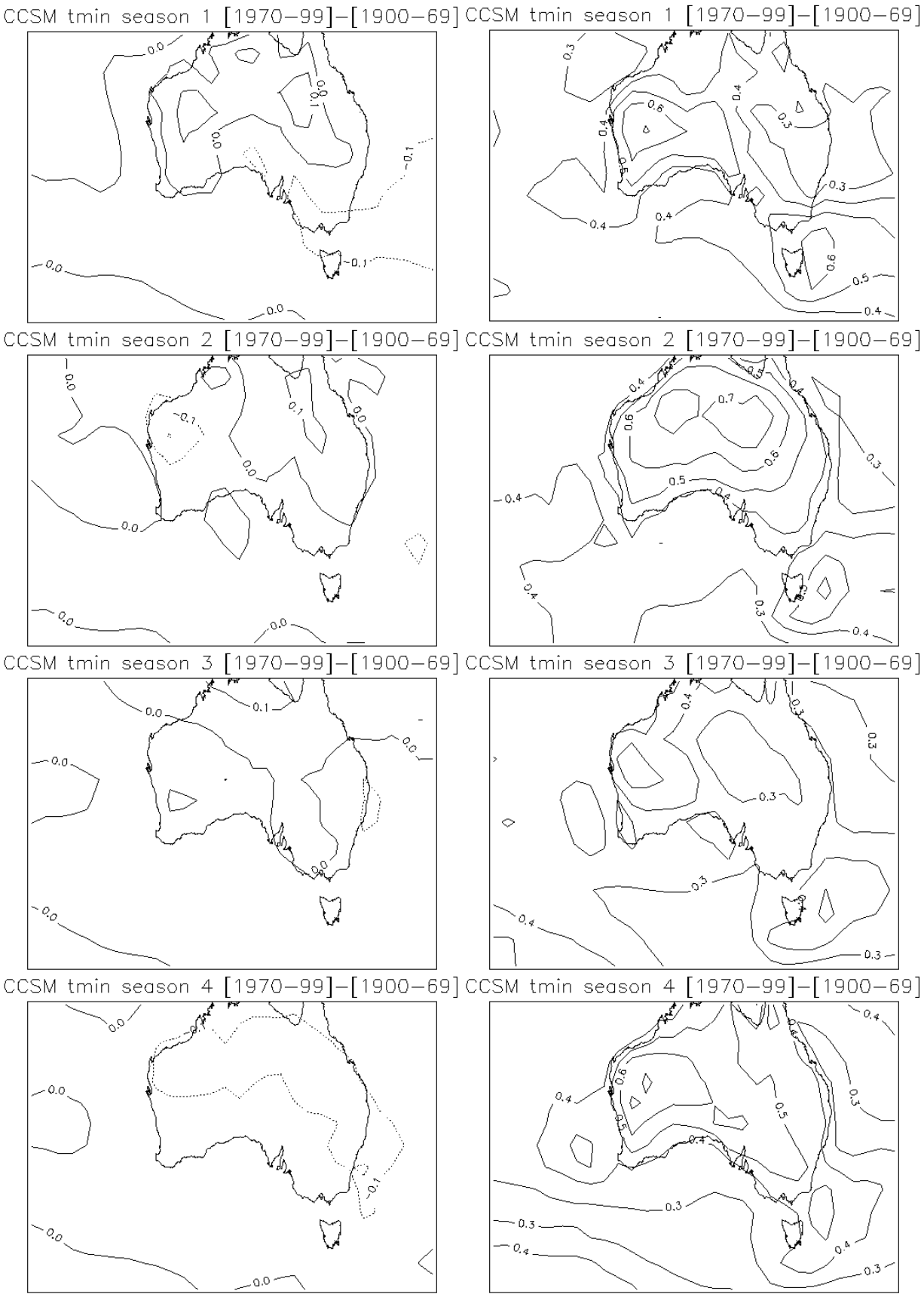

Fig 7: *As per Figure 6 but for minimum Temperature (T_{min}) in °C.*

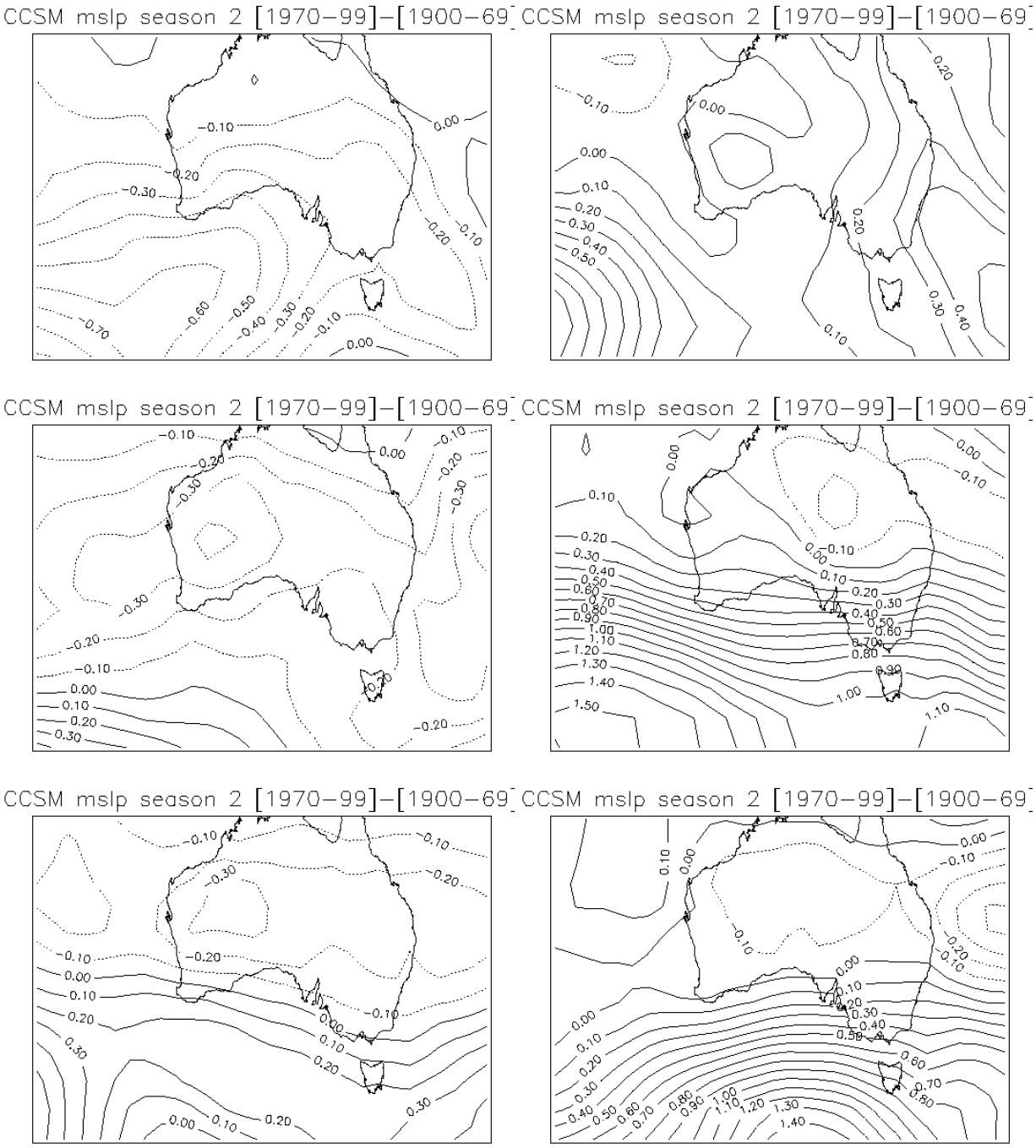

Fig 8: *Maps of differences of summer MSLP (in hPa) between 1970–1999 and 1900–1969, for individual simulations from the natural (top), anthropogenic (middle) and all forcings (lower) ensembles. The left column illustrates the lowest MSLP increase above southern Australia in each ensemble; the right column illustrates the largest MSLP increase.*

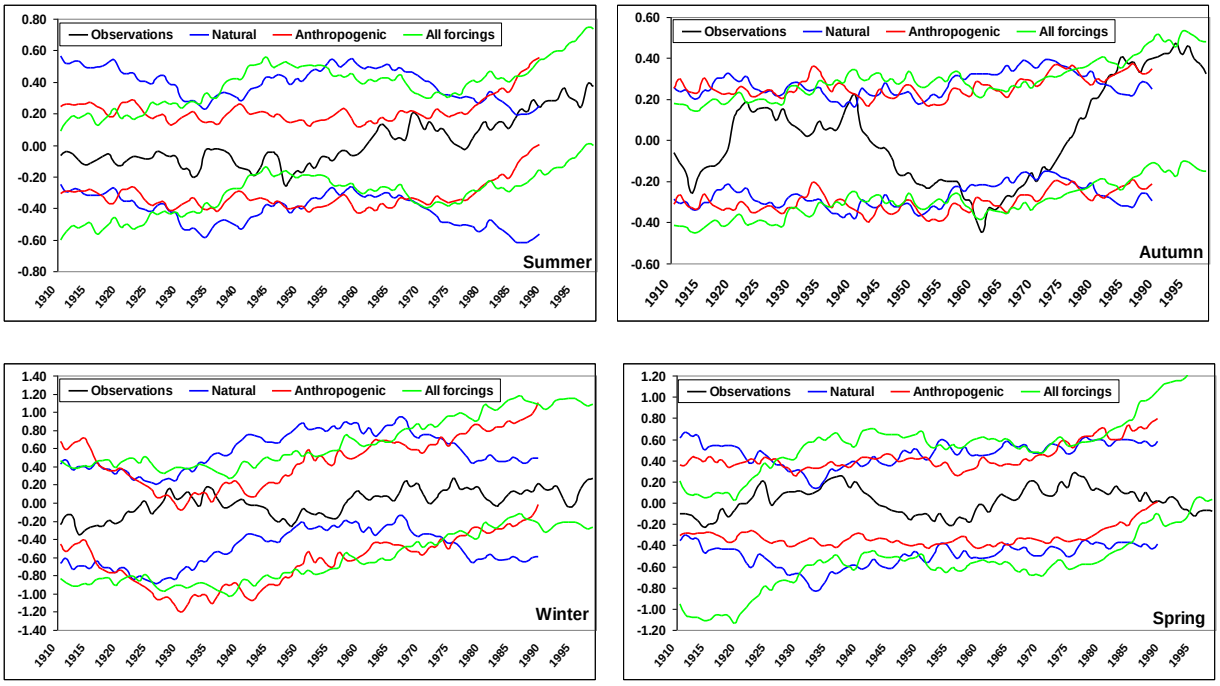

Fig 9: *20-year running average from 1900 of observed MSLP anomalies from the 20th Century climatology (in hPa) across SEA (black line, until 2008); estimates of the uncertainty range from the natural (blue), anthropogenic (red) and full forcings (green) ensemble at the 75 per cent confidence level (see main text for details on the calculations); the full forcings ensemble is extended to 2008 using A2 emission scenario.*

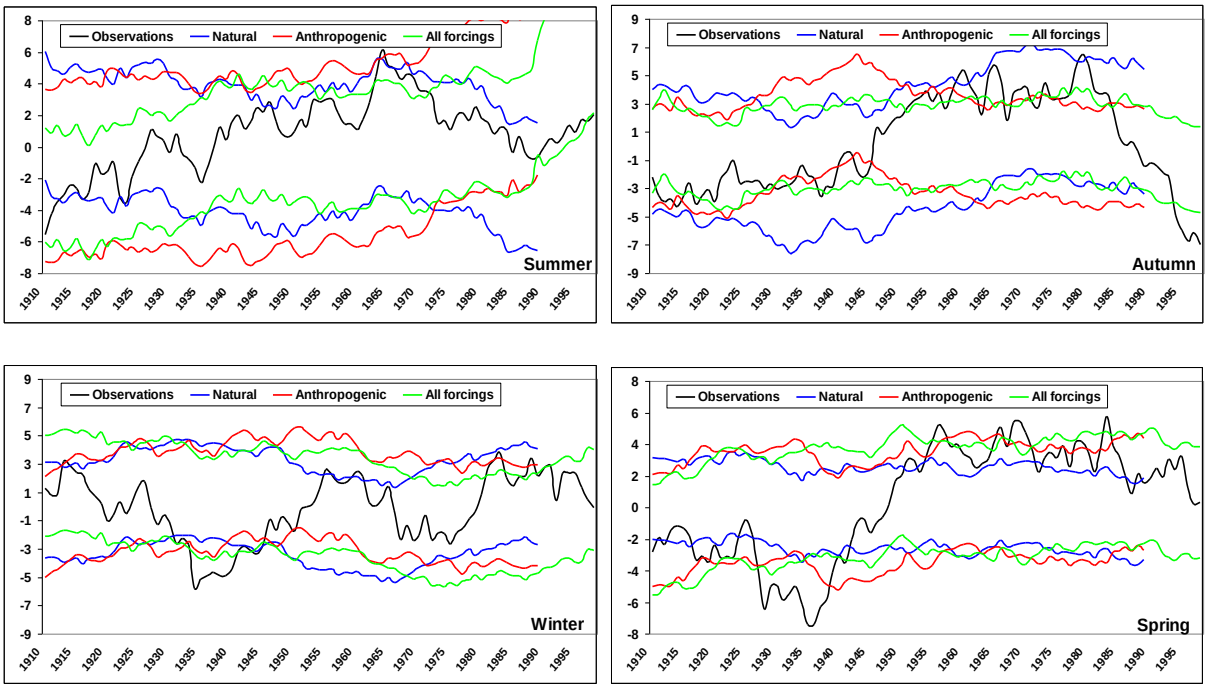

Fig 10: *As per Figure 9 but for precipitation (in mm).*

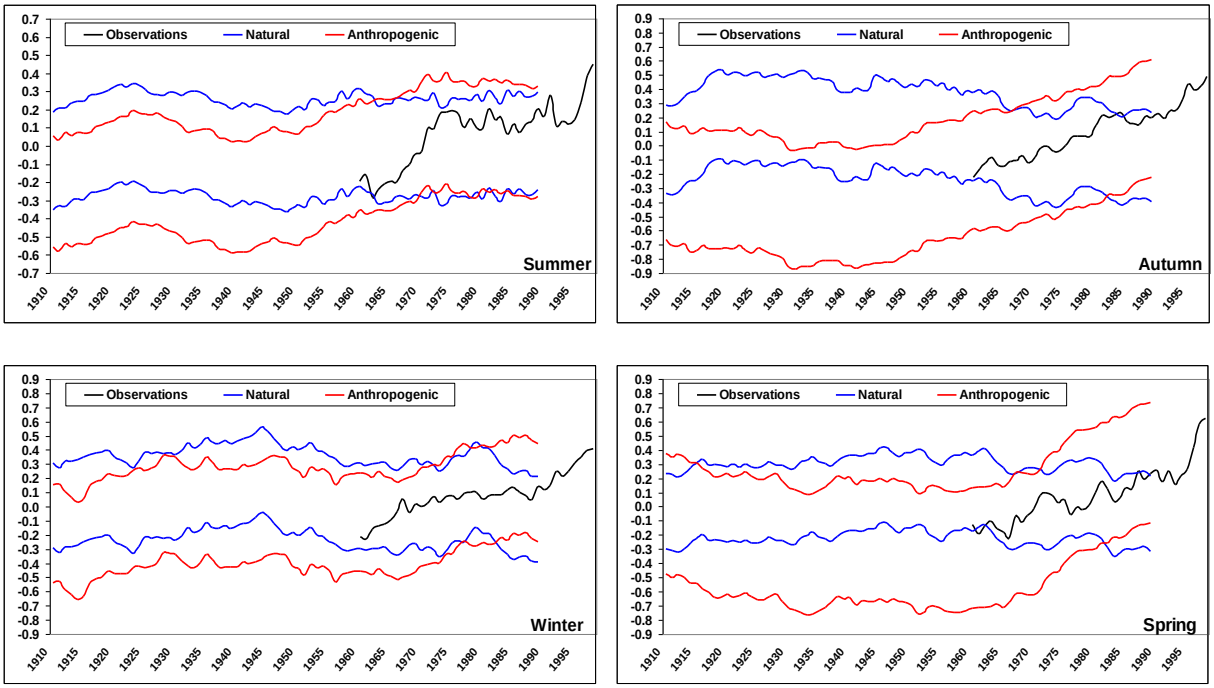

Fig 11: *As per Figure 9 but for T_{max} (in °C). No data are available for the full forcings ensemble.*

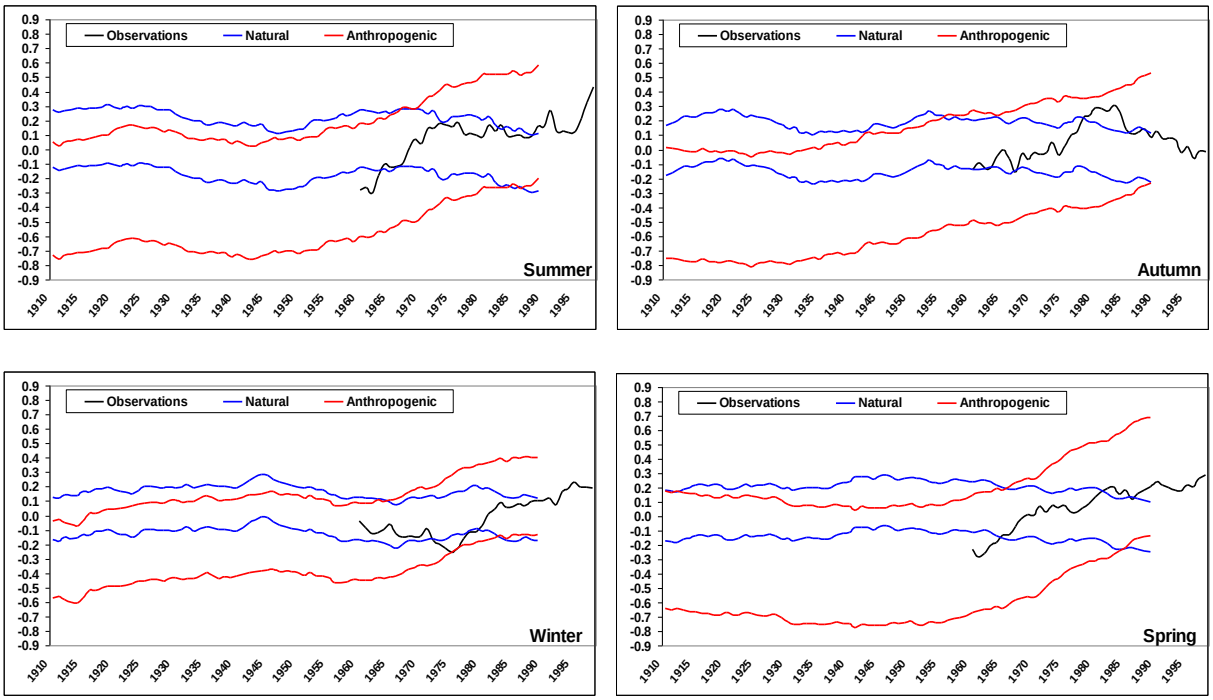

Fig 12: *As per Figure 9 but for T_{min} (in °C).*

Table 2: *Averages across the 164 SWEA rainfall stations of the 20 and 40-years linear trends (in mm.day^{-1} per century) fitted to the observations (left column) and to the downscaled reconstructed series, for each calendar season and each CCSM3 ensemble: with natural external forcings, anthropogenic external forcings and all forcings combined. The full range (min and max) for each ensemble is based on 6 SDMs applied to 5 simulations per ensemble (30 cases).*

		Obs	Natural forcings			Anthropogenic forcings			All forcings combined		
			average	min	max	average	min	max	average	min	max
DJF	60-99	0.05	-0.10	-0.57	0.59	0.09	-0.37	0.75	0.27	-0.31	0.73
	80-99	2.74	0.79	-0.56	2.22	-0.51	-2.21	1.84	0.18	-3.01	1.76
MAM	60-99	-1.23	-0.11	-0.94	0.61	-0.38	-1.34	0.40	-0.61	-1.16	0.11
	80-99	-2.64	-0.05	-2.20	1.55	-0.84	-3.60	0.57	-1.25	-4.43	0.39
JJA	60-99	0.63	0.44	-0.62	1.76	-0.36	-0.98	0.14	-0.15	-0.83	0.39
	80-99	-1.55	0.93	-0.97	5.01	0.23	-1.56	1.70	-0.20	-2.05	1.76
SON	60-99	0.49	0.08	-0.37	0.65	-0.13	-0.82	0.45	-0.06	-0.78	0.73
	80-99	1.93	1.26	-0.52	3.27	-0.15	-2.43	2.39	-0.72	-2.82	0.40

Table 3: *As per table 2 but for the 160 stations in SMD*

		Obs	Natural forcings			Anthropogenic forcings			All forcings combined		
			average	min	max	average	min	max	average	min	max
DJF	60-99	-0.09	-0.20	-1.31	1.38	0.09	-0.78	1.25	0.38	-0.10	0.98
	80-99	2.23	0.65	-2.23	3.95	-2.03	-4.35	0.62	1.35	-1.67	3.70
MAM	60-99	-0.55	0.10	-0.85	1.21	-0.25	-1.02	0.58	-0.29	-0.91	0.61
	80-99	-1.61	1.01	-2.33	4.02	-0.39	-3.76	2.75	-0.82	-3.90	1.85
JJA	60-99	0.73	0.36	-0.71	1.84	-0.02	-0.52	0.56	-0.36	-0.99	0.47
	80-99	-0.71	0.78	-1.01	2.28	0.23	-3.29	2.67	-0.27	-2.99	3.61
SON	60-99	0.28	0.10	-0.93	0.95	0.02	-1.50	1.11	0.06	-0.86	1.01
	80-99	3.83	1.15	-0.79	3.93	-0.10	-3.32	2.84	-1.31	-3.61	0.20

Table 4: *As per table 2 but for T_{max} based on 22 stations in SWEA (in °C per century)*

		Obs	Natural forcings			Anthropogenic forcings			All forcings combined		
			average	min	max	average	min	max	average	min	max
DJF	60-99	0.94	-0.40	-1.76	0.50	0.58	-0.72	1.49	0.91	-0.33	2.29
	80-99	-0.92	0.41	-1.12	2.66	0.00	-3.51	2.84	-0.55	-2.16	0.96
MAM	60-99	1.46	-0.36	-1.51	0.98	0.80	-0.59	2.91	1.56	0.30	3.86
	80-99	-3.10	-0.40	-4.46	4.85	1.53	-1.29	5.28	0.76	-1.96	4.14
JJA	60-99	1.50	0.02	-0.63	0.83	0.46	-0.64	1.40	0.89	0.12	1.40
	80-99	1.84	-0.43	-2.32	0.60	-0.01	-1.83	1.85	0.19	-0.99	1.51
SON	60-99	0.99	-0.37	-1.97	0.87	1.73	0.21	3.38	1.19	-0.40	2.61
	80-99	-2.81	-0.54	-3.21	2.12	1.19	-0.82	3.70	1.49	-2.08	7.42

Table 5: *As per table 3 but for T_{max} based on 19 stations in SMD (in °C per century)*

		Obs	Natural forcings			Anthropogenic forcings			All forcings combined		
			average	min	max	average	min	max	average	min	max
DJF	60-99	1.66	-0.34	-1.09	1.38	-0.02	-0.83	1.17	1.00	-1.00	1.83
	80-99	-3.52	-1.46	-4.73	0.33	0.05	-2.92	2.79	-0.31	-1.69	1.13
MAM	60-99	1.47	-0.25	-1.91	1.48	1.04	-0.49	3.67	1.53	-0.29	3.92
	80-99	-2.05	-1.07	-4.58	4.83	1.25	-2.23	4.57	0.41	-2.71	4.57
JJA	60-99	1.11	-0.01	-1.04	1.08	0.85	-0.47	2.30	1.38	0.29	2.44
	80-99	3.13	-0.61	-3.00	0.71	0.21	-3.45	3.13	0.34	-2.33	3.21
SON	60-99	0.23	-0.67	-2.25	0.87	2.13	0.77	3.60	1.04	-1.45	2.12
	80-99	-5.64	-1.19	-2.35	0.18	0.85	-1.21	4.87	1.54	-3.21	6.45

Table 6: *As per table 4 but for T_{min} in SWEA (in °C per century)*

		Obs	Natural forcings			Anthropogenic forcings			All forcings combined		
			average	min	max	average	min	max	average	min	max
DJF	**60-99**	0.55	-0.25	-1.15	0.48	0.65	0.05	1.52	0.67	-0.53	1.34
	80-99	1.40	0.31	-0.79	1.54	0.83	-1.83	3.71	0.12	-0.92	2.04
MAM	**60-99**	0.26	-0.06	-0.65	0.81	0.44	-0.65	1.04	0.59	-0.60	1.51
	80-99	-4.70	-0.07	-1.61	1.42	0.76	-1.29	2.06	-0.14	-2.34	3.02
JJA	**60-99**	1.44	0.38	-0.55	1.07	0.27	-1.07	0.99	0.59	0.17	1.41
	80-99	1.18	0.54	-0.98	2.60	0.42	-1.13	2.47	0.50	-0.68	1.89
SON	**60-99**	1.20	-0.30	-1.78	0.95	0.72	0.15	1.36	0.50	-0.36	1.30
	80-99	-1.02	-0.40	-2.68	1.58	0.45	-0.55	1.45	0.57	-1.06	3.80

		Obs	Natural forcings			Anthropogenic forcings			All forcings combined		
			average	min	max	average	min	max	average	min	max
DJF	**60-99**	1.02	-0.38	-1.22	0.90	0.20	-1.02	1.37	0.86	-0.48	1.84
	80-99	1.01	-0.92	-2.68	2.37	-0.89	-4.45	1.08	-0.23	-2.34	2.54
MAM	**60-99**	0.12	0.24	-1.35	1.25	0.48	-0.85	1.31	1.34	-0.38	3.62
	80-99	-6.34	0.24	-2.27	3.63	1.36	-0.72	3.53	-0.04	-5.09	4.29
JJA	**60-99**	0.90	0.60	-0.56	1.36	0.41	-0.94	1.57	0.68	-0.29	1.38
	80-99	1.01	1.13	-1.86	4.73	0.53	-1.09	2.07	0.65	-1.65	2.16
SON	**60-99**	0.59	-0.19	-1.35	0.62	1.30	0.32	2.03	0.74	-0.42	1.86
	80-99	-0.35	0.22	-1.54	3.34	0.09	-1.26	1.70	0.56	-1.76	4.41

Table 7: *As per Table 5 but for Tmin in SMD (in °C per century)*

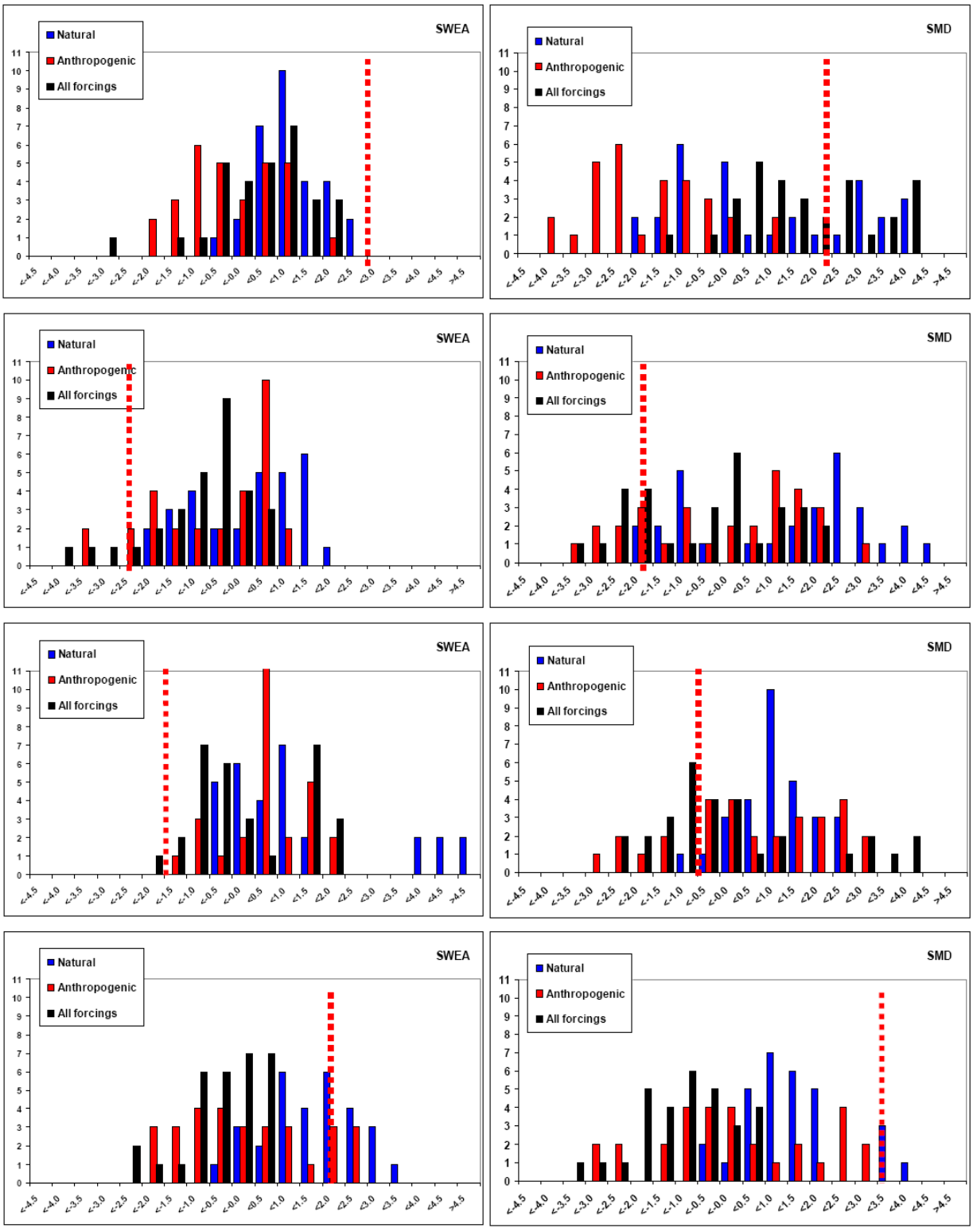

Fig 13: *Histograms (number of cases) of the linear 1980-1999 rainfall trends (in mm.day^{-1} per century) obtained from the downscaling of CCSM3 ensembles (with natural, anthropogenic and combined external forcings) for SWEA (left) and SMD (right) and the four calendar seasons (summer to spring from top to bottom). Observed trends are shown as dashed red line.*

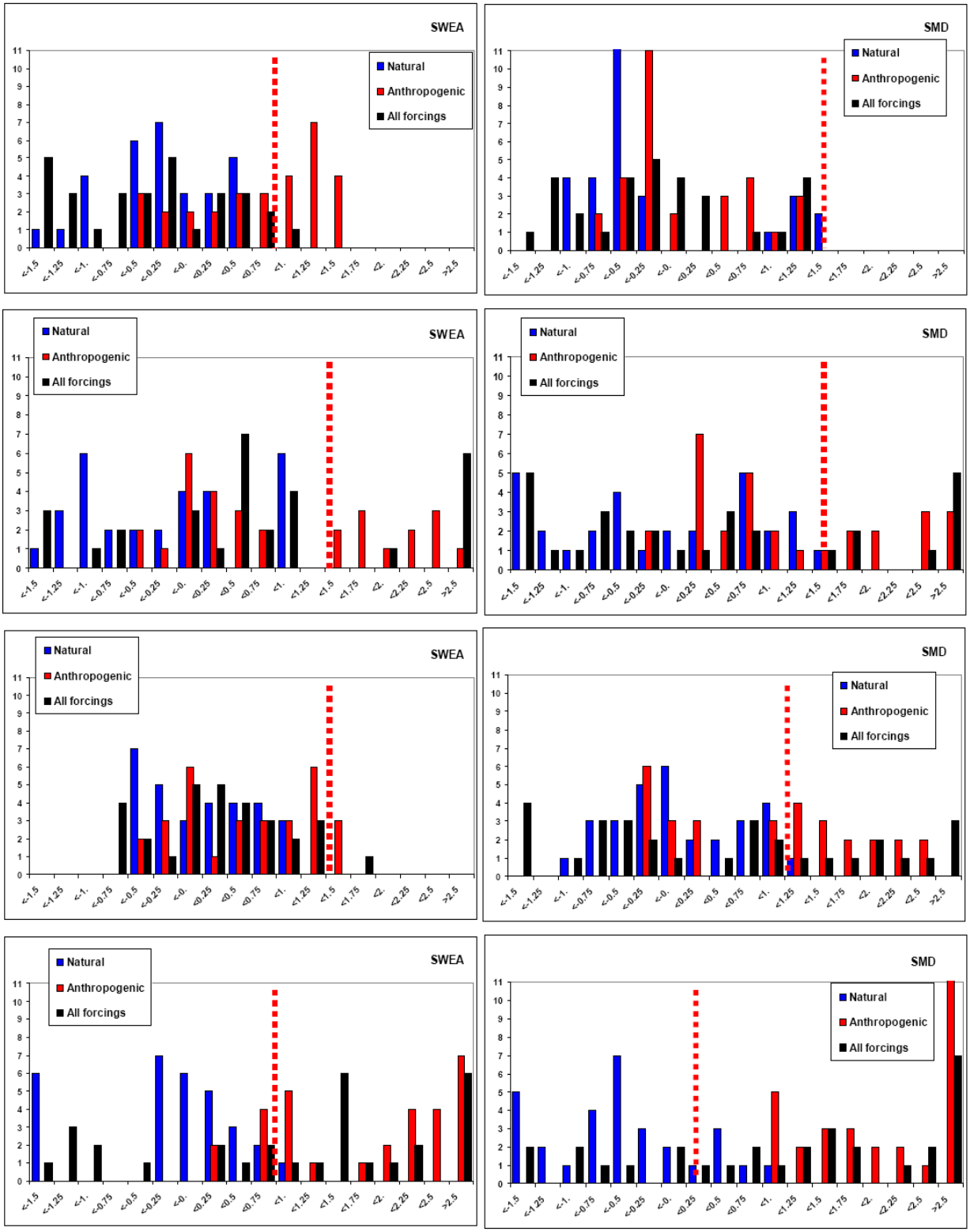

Fig 14: *As per Fig. 13 but for the 1960-1999 T_{max} trends (in °C per century).*

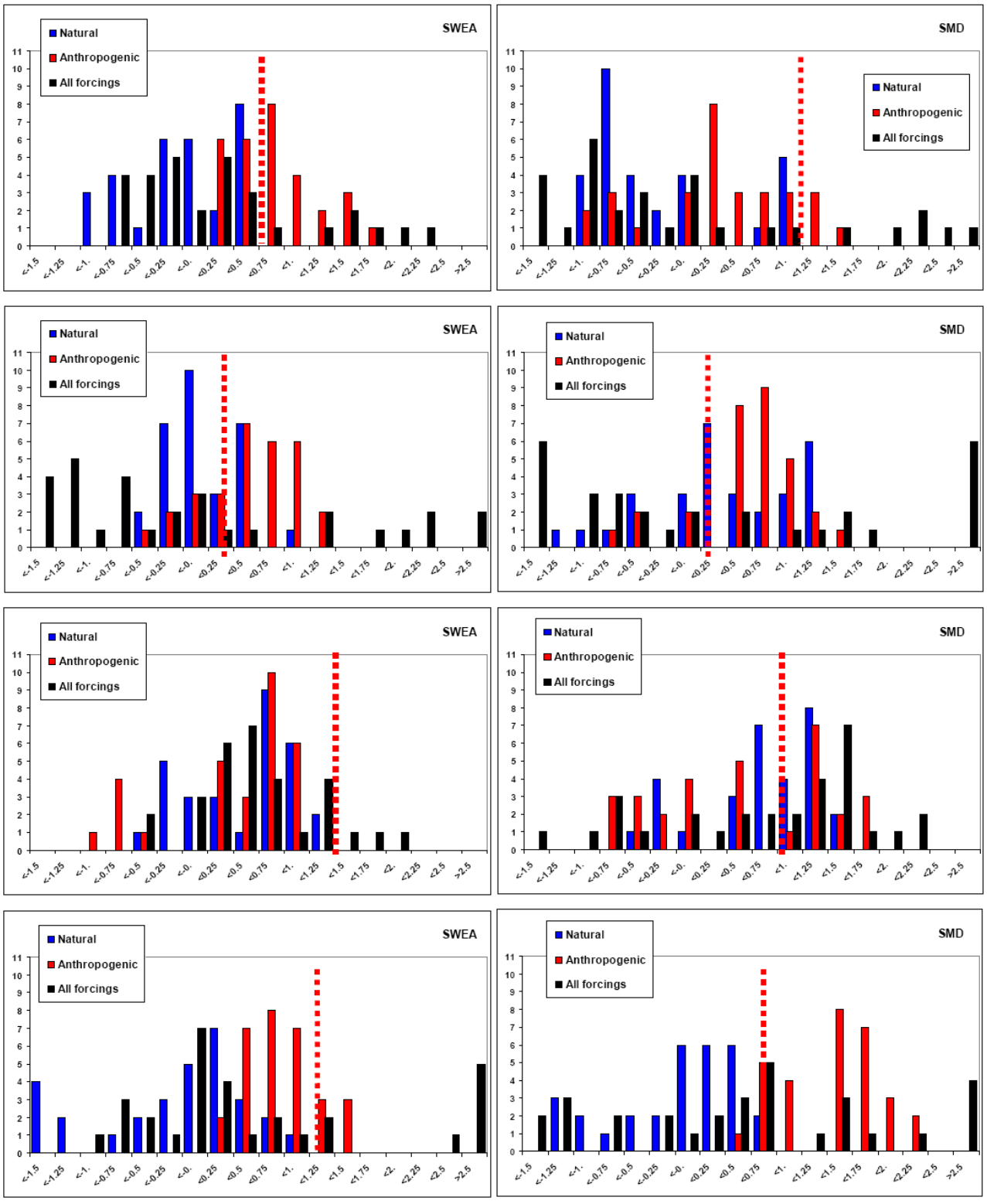

Fig 15: *As per Fig. 14 but for* T_{min}.

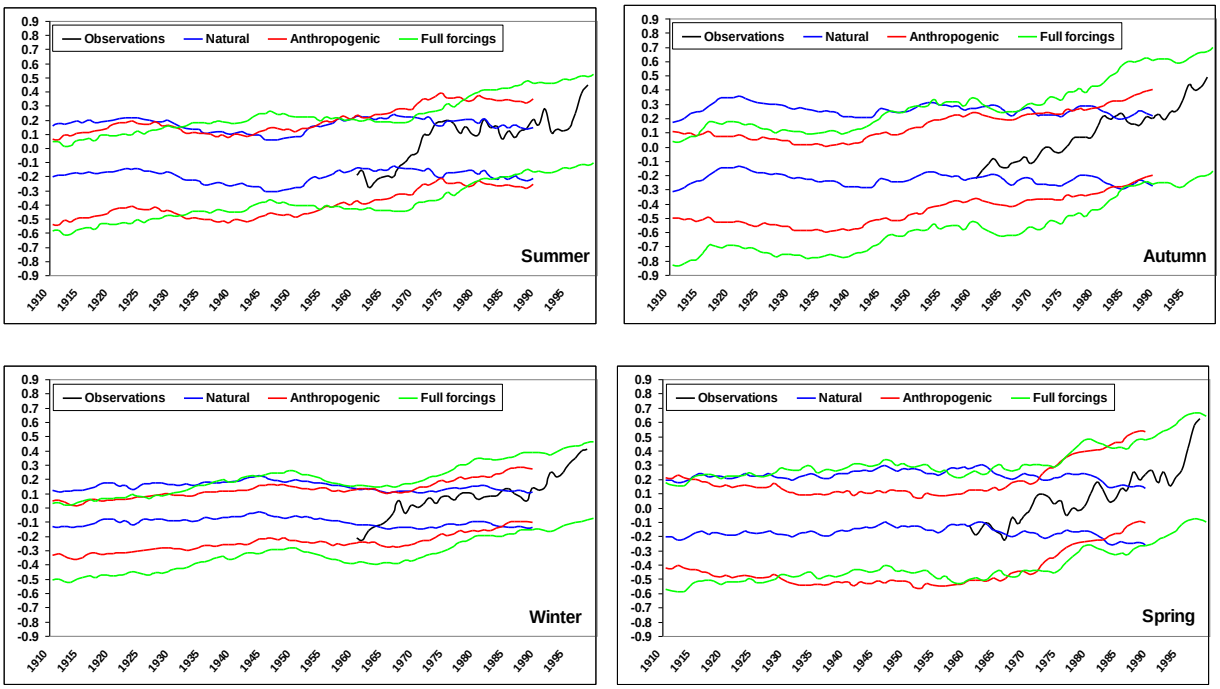

Fig 16: *As per Figure 11 but for downscaled T_{max} series (in °C). The ensemble uncertainty range is based on the 90 percentile instead of the 75 percentile as in Figure 11.*

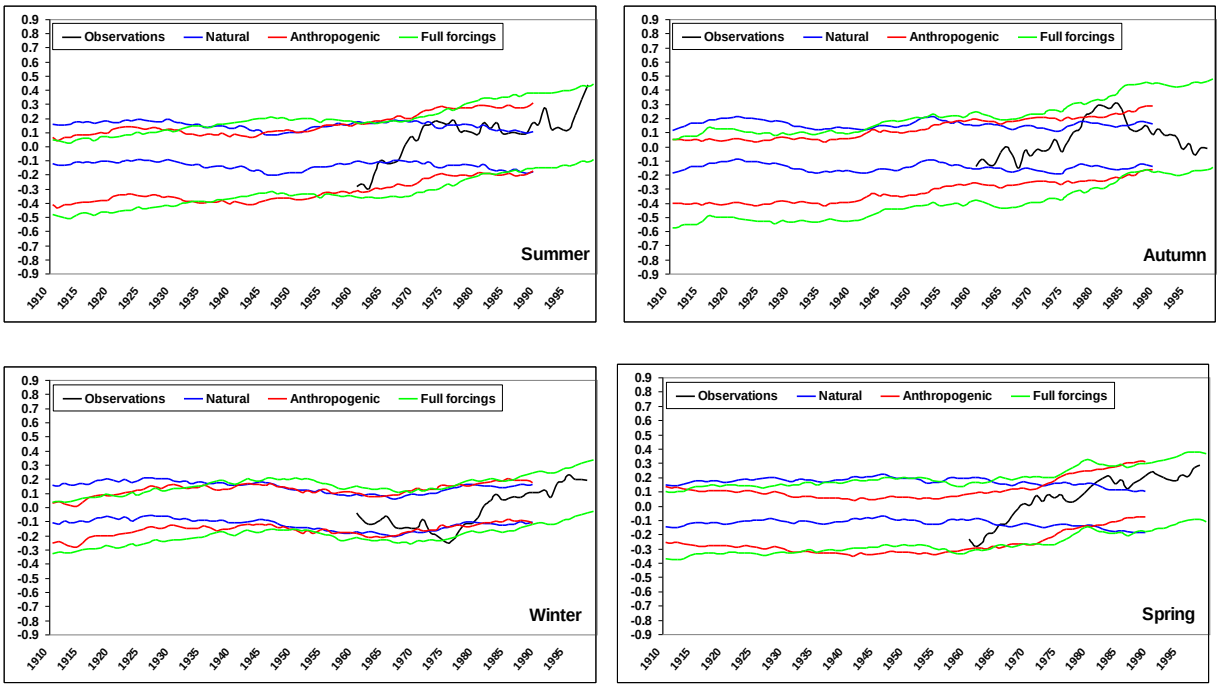

Fig 17: *As per Figure 16 but for T_{min}.*